ADVANCED OPTICAL MATERIALS
www.advopticalmat.de

Highly Directional Emission and Beam Steering from Organic Light-Emitting Diodes with a Substrate Diffractive Optical Element

Shuyu Zhang, Graham A. Turnbull, and Ifor D. W. Samuel**

An interesting challenge in the development of organic light-emitting diodes (OLEDs) is how to control the spatial pattern of their emission, such as the direction of light emission. Directional OLEDs could offer great potential for full resolution autostereoscopic naked-eye 3D displays[1] and visible light communication.[2] In planar OLED structures, a significant fraction of the internal light emission is trapped in guided modes. This trapped light is a major limitation on the external quantum efficiency, and a number of studies have integrated photonic microstructures into OLEDs to improve the device efficiency by extracting trapped light such as the substrate modes,[3] the waveguide modes[4] and the surface plasmon polariton modes[5] into the escape cone. Here we investigated an interesting related problem that has received much less attention, namely how photonic microstructures could be used to achieve high directionality of emission.[6] We have recently reported a solution-processable microstructured OLED with enhanced directionality of emission by embedding a photonic crystal into the organic layers using a simple nano-replication technique.[7] This embedded photonic microstructure gives a compact footprint, but requires a delicate balance between the optimisation of electrical and optical properties.

In this communication we develop photonic microstructured substrates for OLEDs which give enhanced directionality while not interfering with the optimised electrical design of the OLEDs. A nanoimprinted diffractive optical element (DOE) is integrated in the substrate of the OLED adjacent to the emitting pixel, which extracts the directional substrate mode without any Lambertian background. We steer the direction of the emitted beam both by varying the period of the DOE and by bending a flexible DOE substrate. A broadband OLED with a DOE embedded in a waveguide was previously used by Ramuz et al.[8] to make a mini-spectrometer for bio-sensing. Here we achieve highly directional emission using a narrow-linewidth europium (Eu)-based OLED to minimise colour dispersion. The emission out-coupled from the DOE is polarisation-independent and confined in a single narrow emission cone with full-width-half-maximum (FWHM) divergence of around 15° or less. Around 90% of the out-coupled light can be confined within an angle of 20° in the detection plane which is significantly different from the normal Lambertian emission of OLEDs.

In our previous research, we have developed a highly efficient solution-processable Eu-based OLED with commercially available materials.[9] Through careful design of hosts and hole/electron transport layers to balance the charge carriers, we were able to electrically optimise the device efficiency. The resulting device exhibited an external quantum efficiency of 4.3% at a brightness of 100 Cd/m^2. The OLED pixel was 4 mm × 4 mm, centred on the 12 mm × 12 mm glass substrate. The DOE was fabricated on the same type of glass substrate and butt coupled to the edge of the OLED substrate. The DOE pixel was also 4 mm × 4 mm in size and the separation distance between the OLED pixel and the DOE pixel was 8 mm. The device configuration of the DOE-assisted OLED is shown in **Figure 1**a. With this configuration, the optical properties could be independently optimised without compromising the electrical properties of the OLED. The DOE was composed of a 2D square array of pillars in the nanoimprint resist of period of 335 nm and depth of 80~90 nm (see atomic force microscopy (AFM) image in Figure 1b) with an 80 nm-thick layer of silver on top. Several different DOEs were coupled to the OLED, with periods ranging from 275 nm to 365 nm. The angular dependence of the emission from the DOE coupled OLED was measured using the measurement setup shown in Figure 1c. The light was collected by the end of a fibre bundle mounted on a motorised stage. The other end of the fibre was attached to an Andor DV420-BV CCD spectrometer. The DOE was positioned in the rotation centre of the motorised stage and the direct emission of the OLED was blocked by an opaque cover, so only the out-coupled emission from the DOE was collected. The fibre input was scanned in the detection plane to investigate how the substrate DOE affects the directionality of emission. In order to check the beam divergence in the perpendicular direction, the sample was rotated 90° in the substrate plane and tilted with an angle to make sure the peak emission out-coupled from the DOE lies in the detection plane. We refer to the former detection plane before rotation of the sample as 'the horizontal detection plane' and the latter detection plane after rotation as 'the vertical detection plane', as illustrated in Figure 1c.

The electroluminescence spectra of the Eu-based OLEDs have a dominant emission peak at 612 nm with a FWHM of less than 5 nm. In order to explore the direction into which the emitted power is diffracted, the spectral intensity of the angular dependent emission profiles were integrated in a range of 609 nm to 614 nm. In general the emission pattern of planar OLED devices is very close to Lambertian, due to the change of solid angles at the interface of substrate and air,[10]

S. Zhang, Dr. G. A. Turnbull, Prof. I. D. W. Samuel
Organic Semiconductor Centre
SUPA, School of Physics and Astronomy
University of St. Andrews, North Haugh
St. Andrews, Fife KY16 9SS, UK
E-mail: gat@st-andrews.ac.uk; idws@st-andrews.ac.uk

This is an open access article under the terms of the Creative Commons Attribution License, which permits use, distribution and reproduction in any medium, provided the original work is properly cited.

DOI: 10.1002/adom.201300441

© 2014 The Authors. Published by WILEY-VCH Verlag GmbH & Co. KGaA, Weinheim

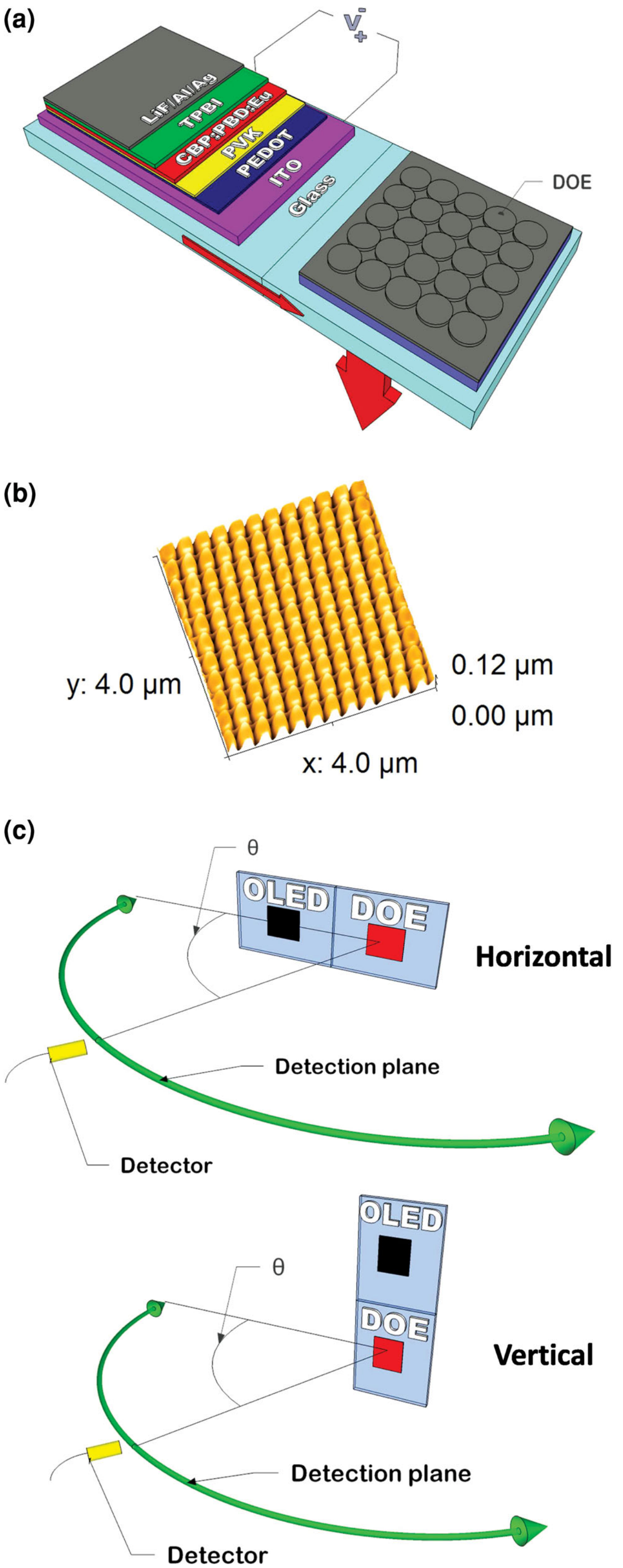

Figure 1. (a) Device configuration of the DOE-assisted OLED; (b) AFM image of the patterned DOE layer, which was patterned by nanoimprint lithography; (c) geometry of measurement of angular dependence of emission.

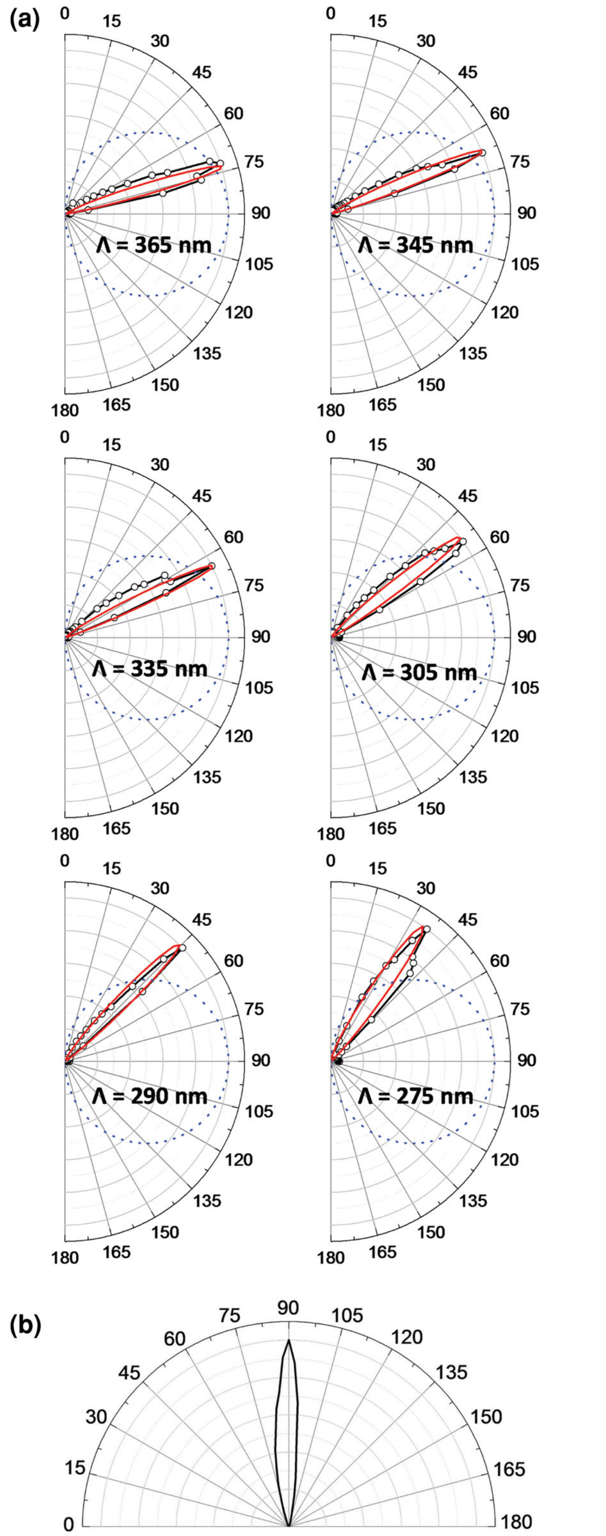

Figure 2. (a) Integrated angular emission profiles of the DOE-assisted OLED in the horizontal detection plane in a range of 609 nm to 614 nm as a function of the grating period of the DOE (black curves and circles represent the experimentally measured results; red curves represent the simulated results of out-coupling the substrate mode; blue dots represent the emission profile of a Lambertian emitter); (b) integrated angular emission profiles of the DOE-assisted OLED in the vertical detection plane.

© 2014 The Authors. Published by WILEY-VCH Verlag GmbH & Co. KGaA, Weinheim
Adv. Optical Mater. 2014,
DOI: 10.1002/adom.201300441

Table 1. A comparison of the fraction of emission (FOE) of the DOE-assisted OLED with that of a Lambertian emitter in an angular range of 20°.

(a) Fraction of emission for a rigid DOE						
Grating period	365 nm	345 nm	335 nm	305 nm	290 nm	275 nm
Angular range (20°)	60~80°	54~74°	48~68°	40~60°	30~50°	24~ 44°
DOE-assisted OLEDs	89%	88%	90%	87%	90%	92%
Lambertian emitter	18%	17%	16%	15%	12%	11%

(b) Fraction of emission for a flexible DOE			
	Without Bending	Bending outward (+21°)	Bending inward (–17°)
Angular range (20°)	58~78°	78~98°	46~66°
DOE-assisted OLEDs	81%	82%	91%
Lambertian emitter	18%	19%	16%

however, the emission pattern of the light coupled out of the DOE was strongly changed to a beam of narrow angular divergence. **Figure 2**a shows the angular emission in the horizontal detection plane from the DOE-assisted OLEDs, as a function of the grating period of the DOE (black curves and circles). The emission profile of a Lambertian emitter (blue dots) is shown for comparison. The observation angles 0° and 180° are parallel to the surface of the substrate, while 90° is the observation angle normal to the surface. The results shown are for measurements without a polariser; however, s- and p-polarisations give very similar emission patterns. For each DOE used, the light was emitted as a narrow beam of FWHM divergence around 15° or less. The peak power was detected at angles of 72°, 68°, 64°, 54°, 46° and 36°, corresponding to grating periods of 365 nm, 345 nm, 335 nm, 305 nm, 290 nm and 275 nm respectively. The grating period of the DOE controls the emitting direction in this detection plane.

In order to assess the increase in beam directionality, we define a parameter called the fraction of emission (FOE) given by the percentage of emitted power integrated in a specified range of angles in the detection plane. **Table 1**a shows a comparison of the FOE of the DOE-assisted OLED with that of a Lambertian emitter in an angular range of 20°. A Lambertian emitter shows a FOE of around 11% to 18% depending on how close the centre of the angular range is to the surface normal, whereas the DOE-assisted OLED can achieve a FOE of around 90% no matter where the centre of the angular range locates. This means around 90% of the emitted power was confined in this angular range in the horizontal detection plane.

To investigate the emission profile in the orthogonal direction, the fibre was first moved to the peak position of the emission power in the horizontal detection plane and then the fibre was moved in the vertical plane. Figure 2b shows the results of the measured angular emission in the vertical detection plane. The FWHM beam divergence of the emission was around 13°. We note that the beam divergence is dependent on the distance between the OLED pixel and the DOE pixel and analyse this quantitatively in Supporting Information. The FWHM of out-coupled emission depends on the range of in-plane wavevectors in the substrate that are collected by the DOE, which itself depends on the separation between the OLED pixel and the DOE pixel. As the separation increases, the angular range of in-plane wavevectors becomes smaller. So a higher directionality of emission will be achieved in this case. Clearly this comes with a compromise of light intensity because the DOE receives a smaller fraction of the substrate wave, and a balance between light intensity and directionality should be considered. In our configuration, the diffraction efficiency of the 2D square array grating is roughly 20% in s-polarisation and 50% in p-polarisation, estimated by simulation. The ratio of the light out-coupled by the DOE over the light directly emitted through the bottom substrate is around 8%, which was measured by luminous meter and power meter. This ratio can be further improved by implanting more DOEs with appropriate grating vectors around the OLED to make use of more light from the substrate mode.

Since the out-coupled emission from the DOE is confined in both orthogonal detection planes, it is a truly confined 'beam' emitting from the DOE into the free space. This is quite different from the general angular distribution of emission from OLEDs with embedded wavelength-scale gratings.[11] The emission out-coupled from the latter generally forms a symmetric cross shape for a typical 2D square array grating rather than becomes truly confined in a long narrow cone. In addition, the polarisation independence of the emission profiles of the DOE-assisted OLED is quite different from other OLEDs with internal spatial modification of emission. Another conceivable strategy would be placing a transparent DOE directly over the OLED pixel, but in addition to any diffraction of waveguided modes, the range of emission angles of the OLED would lead to a spatially broad background emission.

Simulations were next carried out in order to trace the origin of directional emission. The Transfer Matrix method was first used to calculate the modes trapped in the substrate.[12] Using the measured angular emission profiles of planar Eu-based OLED in s- and p-polarisation, the profile of the recombination zone and the emitting dipole orientation were first determined using a least-squares fitting algorithm.[13] Then the information of the light intensity trapped in the substrate as a function of k vector was extracted. The model includes self-absorption and optical anisotropy, with the complex refractive indices of all layers measured and fitted by ellipsometry. The second step was to simulate the DOE structure using a commercial modelling software COMSOL Multiphysics v4.3. COMSOL uses the finite element method to solve Maxwell's equation in the Wave Optics module. According to the calculation, only one diffraction order can be out-coupled into the escape cone by the DOE and the diffraction efficiency as a function of k vector can be obtained.

© 2014 The Authors. Published by WILEY-VCH Verlag GmbH & Co. KGaA, Weinheim

ADVANCED OPTICAL MATERIALS
www.advopticalmat.de
www.MaterialsViews.com

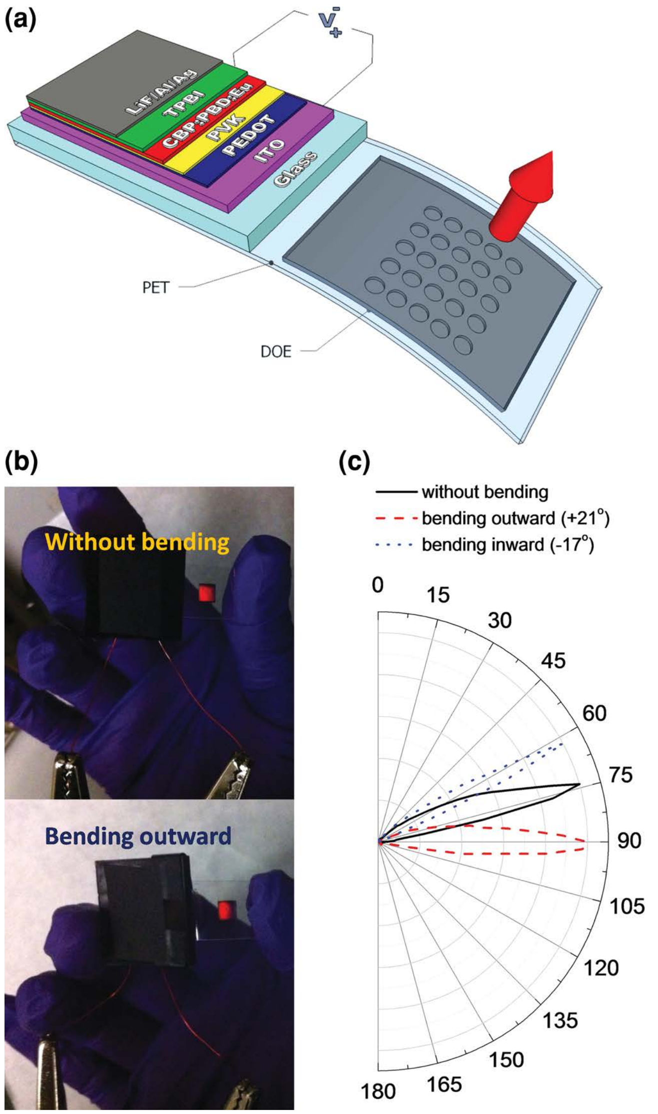

Figure 3. (a) Device configuration of the flexible DOE-assisted OLED; (b) photos of the emission from the DOE-assisted OLED with and without bending the flexible substrate; (c) angular dependent emission profiles of the DOE-assisted OLED in the horizontal detection plane when the flexible substrate was bent to different directions (inward/outward).

The last step was to calculate the change of the solid angle from the substrate into the free space. The simulated results are plotted in Figure 2a in red curves. Here we only consider the out-coupling of the substrate mode. The experimental and simulation results are in good agreement, which indicates most of the out-coupled emission can be attributed to the out-coupling of the substrate modes.

The ease or complexity of changing the direction of the beam is another import aspect. Since the direction of the beam out-coupled by the rigid DOE is fixed by the grating period of the DOE, we also developed a flexible DOE which can simply change the beaming direction by bending the flexible substrate relative to the OLED. **Figure 3**a shows the device configuration of the flexible DOE-assisted OLED. The flexible substrate was made of polyethylene terephthalate (PET) and attached to the glass substrate of the OLED with index matching oil. Figure 3b shows the photos of the emission from the DOE-assisted OLED with and without bending the flexible substrate. The emission peak shifted to a different observing angle when the flexible substrate was bent. Figure 3c shows the angular dependent emission profiles of the DOE-assisted OLED in the horizontal detection plane when the flexible substrate was bent to different directions (inward/outward). The beam was still well confined regardless of the bending and the FWHM beam divergence was around 9° to 14°. Table 1b shows the comparison of the FOE of the flexible DOE-assisted OLED with that of a Lambertian emitter in an angular range of 20°. The FOE of the flexible DOE-assisted OLED can also be as high as 80~90%, which indicates the flexible DOE can allow simple changes of the beaming direction without compromising its confinement.

In conclusion, we have developed DOE-assisted OLEDs which give highly directional emission by out-coupling the substrate mode from an efficient solution-processable Eu-based OLED. The polarisation-independent emitted power is confined in a narrow emission cone with FWHM divergence of around 15° or less, which distinguishes itself from other OLEDs with spatial modification of emission. Around 90% of the out-coupled light can be confined within an angle of 20° in the detection plane which is significantly different from a Lambertian emitter. A flexible substrate DOE was also developed to simplify the change of beaming direction by bending the flexible substrate without changing the grating periods of the DOE. Our current configuration gives a ratio of the light out-coupled by the DOE to the light directly emitted through the bottom substrate of around 8%. This can be further improved by coupling more of the direct emission of the OLED into the substrate, or by changing the aspect ratio of the substrate. Our approach gives a powerful way of controlling the direction of the emission of OLEDs for applications in displays, communications and lighting.

Experimental Section

The device structure of the Eu-based OLED was glass/indium tin oxide (ITO)/poly(3,4-ethylenedioxythiophene):poly(styrenesulfonate) (PEDOT:PSS)/poly(*N*-vinylcarbazole) (PVK)/4,4′-*N,N*′-dicarbazole-biphenyl (CBP):2-(*tert*-butylphenyl)-5-biphenylyl-1,3,4-oxadiazole (PBD):tris(dibenzoylmethane)mono(4,7-diphenylphenanthroline) europium(III) ($Eu(DBM)_3Bphen$)/1,3,5-tris(2-*N*-phenylbenzimidazolyl) benzene (TPBI)/LiF/Al. The experimental conditions of making Eu-based OLEDs were described in detail previously.[9] The nanoimprint resist was mr-UVCur06 deposited on an adhesion layer of mr-APS1, the thickness of which was 240 nm and 10 nm respectively at the spin-coating speed of 3000 rpm and 4000 rpm. The grating was imprinted using an EVG620 mask aligner with custom UV-NIL toolings. An 80 nm thick silver layer was deposited onto the patterned resist in a vacuum evaporation system after the nanoimprint lithography was completed. For the fabrication of the flexible DOE, a 300 nm TPBI layer was deposited in a vacuum evaporation system first and solvent assisted microcontact moulding was then used to transfer the grating pattern reliably from the silicon master to the TPBI in air. A silver layer was then evaporated on top of the patterned TPBI layer. The angular emission was collected with an interval of 2° in this experiment.

© 2014 The Authors. Published by WILEY-VCH Verlag GmbH & Co. KGaA, Weinheim

DOI: 10.1002/adom.201300441

Supporting Information

Supporting Information is available from the Wiley Online Library or from the author.

Acknowledgements

This work was supported by the Engineering and Physical Sciences Research Council grants "Challenging the limits of photonics: structured light" EP/J01771X and "Ultra-parallel visible light communications" (EP/K00042X). S. Zhang was supported by the Scottish Universities Physics Alliance (SUPA). Underlying research materials can be accessed by contacting the corresponding authors. The authors would like to thank Dr Georgios Tsiminis for the design of the silicon master structures and thank Dr Yue Wang for help with the fabrication of the elastomeric moulds.

Received: October 24, 2013
Revised: November 22, 2013
Published online:

[1] D. Fattal, Z. Peng, T. Tran, S. Vo, M. Fiorentino, J. Brug, R. G. Beausoleil, *Nature* **2013**, *495*, 348.
[2] H. Elgala, R. Mesleh, H. Haas, *IEEE Commun. Mag.* **2011**, *49*, 56.
[3] a) S. Jeon, J. W. Kang, H. D. Park, J. J. Kim, J. R. Youn, J. Shim, J. H. Jeong, D. G. Choi, K. D. Kim, A. O. Altun, S. H. Kim, Y. H. Lee, *Appl. Phys. Lett.* **2008**, *92*, 223307; b) J.-B. Kim, J.-H. Lee, C.-K. Moon, S.-Y. Kim, J.-J. Kim, *Adv. Mater.* **2013**, *25*, 3571; c) Y. Sun, S. R. Forrest, *J. Appl. Phys.* **2006**, *100*, 073106.
[4] a) T. Bocksrocker, F. Maier-Flaig, C. Eschenbaum, U. Lemmer, *Opt. Express* **2012**, *20*, 6170; b) J. Hauss, T. Bocksrocker, B. Riedel, U. Lemmer, M. Gerken, *Opt. Express* **2011**, *19*, A851; c) W. H. Koo, S. M. Jeong, F. Araoka, K. Ishikawa, S. Nishimura, T. Toyooka, H. Takezoe, *Nat. Photonics* **2010**, *4*, 222; d) W. H. Koo, W. Youn, P. F. Zhu, X. H. Li, N. Tansu, F. So, *Adv. Funct. Mater.* **2012**, *22*, 3454; e) X.-L. Zhang, J. Feng, J.-F. Song, X.-B. Li, H.-B. Sun, *Opt. Lett.* **2011**, *36*, 3915; f) J. M. Ziebarth, A. K. Saafir, S. Fan, M. D. McGehee, *Adv. Funct. Mater.* **2004**, *14*, 451; g) W. H. Koo, Y. Zhe, F. So, *Adv. Opt. Mater.* **2013**, *1*, 404.
[5] a) J. M. Lupton, B. J. Matterson, I. D. W. Samuel, M. J. Jory, W. L. Barnes, *Appl. Phys. Lett.* **2000**, *77*, 3340; b) B. J. Matterson, J. M. Lupton, A. F. Safonov, M. G. Salt, W. L. Barnes, I. D. W. Samuel, *Adv. Mater.* **2001**, *13*, 123; c) C. J. Yates, I. D. W. Samuel, P. L. Burn, S. Wedge, W. L. Barnes, *Appl. Phys. Lett.* **2006**, *88*, 161105.
[6] a) J. Feng, T. Okamoto, S. Kawata, *Appl. Phys. Lett.* **2005**, *87*, 241109; b) T. Tsutsui, N. Takada, S. Saito, E. Ogino, *Appl. Phys. Lett.* **1994**, *65*, 1868.
[7] S. Zhang, G. A. Turnbull, I. D. W. Samuel, *Appl. Phys. .Lett* **2013**, *103*, 213302.
[8] a) M. Ramuz, L. Burgi, R. Stanley, C. Winnewisser, *J. Appl. Phys.* **2009**, *105*, 084508; b) M. Ramuz, D. Leuenberger, R. Pfeiffer, L. Burgi, C. Winnewisser, *Eur. Phys. J.-Appl. Phys.* **2009**, *46*, 12510.
[9] S. Zhang, G. A. Turnbull, I. D. W. Samuel, *Org. Electron* **2012**, *13*, 3091.
[10] N. C. Greenham, R. H. Friend, D. D. C. Bradley, *Adv. Mater.* **1994**, *6*, 491.
[11] L. Tutt, J. E. Revelli, *Opt. Lett.* **2008**, *33*, 503.
[12] a) H. Benisty, R. Stanley, M. Mayer, *J. Opt. Soc. Am. A* **1998**, *15*, 1192; b) Z. B. Wang, M. G. Helander, X. F. Xu, D. P. Puzzo, J. Qiu, M. T. Greiner, Z. H. Lu, *J. Appl. Phys.* **2011**, *109*, 053107.
[13] a) M. Flammich, M. C. Gather, N. Danz, D. Michaelis, A. H. Brauer, K. Meerholz, A. Tunnermann, *Org. Electron* **2010**, *11*, 1039; b) S. L. M. van Mensfoort, M. Carvelli, M. Megens, D. Wehenkel, M. Bartyzel, H. Greiner, R. A. J. Janssen, R. Coehoorn, *Nat. Photonics* **2010**, *4*, 329.

© 2014 The Authors. Published by WILEY-VCH Verlag GmbH & Co. KGaA, Weinheim